Role of lateral forces on atom manipulation process on Si(111)-(7 × 7) surface in dynamic force microscopy

Ayhan Yurtsever,[1,2,3,*] Masayuki Abe,[3] Seizo Morita,[1,2] and Yoshiaki Sugimoto[1,4]

[1]*Graduate School of Engineering, Osaka University, 2-1 Yamada-Oka, Suita, Osaka 565-0871, Japan*

[2]*Institute of Scientific and Industrial Research, Osaka University, 8-1 Mihogaoka, Ibaraki, Osaka 567-0047, Japan*

[3]*Graduate School of Engineering Science, Osaka University, 1-1 Machikaneyama, Toyonaka, Osaka 560-0043, Japan*

[4]*Department of Advanced Materials Science, Graduate School of Frontier Sciences, University of Tokyo, 5-1-5, Kashiwanoha, Kashiwa, Chiba 277-8561, Japan*

(Received 1 August 2017; published 5 October 2017)

We investigated the role of lateral force components on the lateral manipulation of intrinsic Si adatoms toward a vacancy site on a Si(111)-(7 × 7) surface using noncontact atomic force microscopy at room temperature. Lateral atom manipulation was accomplished via constant-height scans using a set of tips with varying chemical reactivities. We determined the vertical and lateral force as well as the interaction energy profiles associated with the lateral manipulation of a Si adatom on a Si(111)-(7 × 7) surface. Our results demonstrate that lateral forces do not play a decisive role in the manipulation process while the vertical force component is key for the manipulation process, and the ability to manipulate the Si adatom depends primarily on the chemical nature of the tip apex. Our results further reveal that the tips that exhibit high chemical reactivity with Si adatoms have a sharper interaction energy profile above Si adatoms than tips with less chemical reactivity, indicating the stronger atom-trapping ability of the chemically reactive tips. This characteristic property gives tips the ability to create localized reductions in the energy barrier required for adatom movement, thereby enabling thermally induced adatom hopping toward the tip. These findings can enhance our understanding of the underlying mechanisms involved in the lateral manipulation of intrinsic adatoms of semiconductor surfaces, as well as adsorbate atoms/molecules forming covalent bonds with tip-surface systems, i.e., chemisorption systems.

DOI: 10.1103/PhysRevB.96.155412

I. INTRODUCTION

One of the most promising applications of scanning probe microscopy involves the possibility of creating artificial nanostructures on an atomic scale in a controlled manner. While previous manipulation experiments have relied mostly on scanning tunneling microscopy (STM) and had to be performed on conducting substrates and at cryogenic temperatures [1–4], noncontact atomic force microscopy (NC-AFM) has recently been proven to be an exceptionally powerful and convenient tool for the manipulation of individual atoms [5–16] and molecules [17–23] both vertically and laterally at room temperature as well as at low temperatures. Moreover, NC-AFM has provided the opportunity to realize atomic and molecular manipulation on the surfaces of insulating bulk materials that were not accessible by the STM method [24–29].

More importantly, NC-AFM offers the possibility of measuring the interaction forces and energies involved in the atom manipulation processes [5,7], thereby providing more insights into the underlying mechanisms and information relevant to the nature of interaction between the adsorbate atoms/molecules and the substrate surface. A precise quantification of the lateral forces needed to manipulate metal adsorbates on metallic surfaces at 5 K was accomplished by Ternes *et al.* [7]. The results of this study revealed that the manipulation process is governed mainly by the lateral force component and that the threshold force remains constant, independent of the vertical interaction forces. The method introduced by Ternes *et al.* [7] has been further extended to other adsorbate/surface systems [19,21,22,30,31]. The lateral critical force required to remove a H_2Pc (metal-free phthalocyanine) molecule from its self-assembled network formed on a Pb(111) surface was determined through molecular manipulation in a previous study [19]. Another study determined the lateral and vertical tip-molecule force profiles during the lateral manipulation of a single PTCDA (3,4,9,10-perylene-tetracarboxylicacid-dianhydride) molecule on an Ag(111) surface in the repulsive tip-molecule interaction regime [21,30]. More recently, the mechanochemical response of two conformers of a large organic molecule on a metal surface was investigated by Jarvis *et al.* [22]. The conformational dependence of the lateral force threshold has been identified by measuring the lateral critical forces required to manipulate each conformer, offering the intriguing possibility of studying the mechanical properties of molecular conformers at solid surfaces.

Several theoretical studies have also been performed to clarify the underlying atomic mechanisms governing the manipulation processes for a variety of systems [5,6,12,32–40], which have substantially advanced our understanding of the triggering mechanisms that induce the atomic motion in the manipulation processes. The main mechanism responsible for atomic movement in the attractive tip-sample interaction regime has been attributed to local energy barrier reduction induced by interaction forces between the tip and target atom at the surface [5,33,34,38–40].

Despite these significant achievements, the nature and role of tip-sample interactions as well as tip-apex structural and chemical characteristics in the atomic and molecular manipulation processes are still the subject of debate and

*ayhan.yurtsever@stec.es.osaka-u.ac.jp

investigation [31,39,41–43]. The role of the orbital alignment between the tip and a semiconductor surface in the vertical atom manipulation process was discussed on the basis of density functional theory (DFT) calculations [43], and the effect of different tip terminations on lateral manipulation of a CO molecule on a Cu(111) surface was recently investigated by Emmrich *et al.* [31]. Contrary to the previous findings [7], this latter work revealed that the nature of the tip-apex termination determines the lateral manipulation force threshold for an adsorbate on a metal surface, thus confirming that the presence of the tip helps to lower the energy barrier of the natural atomic diffusion due to the vertical force interaction. In a recent combined NC-AFM and DFT study [39], we addressed the role of tip chemical reactivity on the lateral atom manipulation of intrinsic Si adatoms toward a vacancy site on a Si(111)-(7 × 7) surface at room temperature (RT). We found that the ability to reduce the energy barrier associated with the Si adatom movement depends strongly on tip-apex chemical reactivity. Although much has been learned from these studies about the mechanisms of the various manipulation processes, the relation between the mechanical atom manipulation process on semiconductor surfaces and the role played by the lateral component of the interaction force still remains an open question. More importantly, while the critical role of tip chemical reactivity in the process of energy barrier reduction was well demonstrated in our earlier study based on DFT calculations [39], direct experimental evidence providing an explanation for the interplay between the extent of tip chemical reactivity and the level of energy barrier reduction is still missing and is sorely needed. In these respects, the present study is complementary to our previous work [39].

In the present study, to investigate the role of the lateral force component on the manipulation process, we carried out lateral manipulation of intrinsic Si adatoms toward a vacancy site on a Si(111)-(7 × 7) surface by NC-AFM with different tips varying in chemical reactivity at RT. We determined the vertical and lateral force together with the interaction energy profile acting on the tip over its trajectory along the manipulation path. We found that the lateral force exerted by the tip on the adatom does not play a decisive role on the manipulation of a Si adatom on a Si(111)-(7 × 7) surface. Contrary to the case for metal surfaces [7], the vertical force component is the key to the manipulation process on semiconductors. This striking difference can reasonably be attributed to the fact that the diffusion energy barrier on semiconductors is much larger than that on metals due to the presence of highly directional covalent bonds on semiconductor surfaces, in contrast to the nondirectional bonds on metals with delocalized valance electronic charge.

We also revealed the effect of tip chemical reactivity in the manipulation process. We found that tips with high chemical reactivity possess a sharper interaction energy profile on Si adatoms than the less reactive tips, suggesting that the chemically reactive tips hold a strong atom trapping ability. In other words, the chemically reactive tips have the ability to locally reduce the energy barrier required for adatom diffusion, thereby enabling adatom displacement toward the tip. These findings together can provide an explanation for the observed dependency on tip-apex chemical reactivity of manipulation processes carried out on semiconductors and other surfaces with strongly localized dangling-bond states.

II. EXPERIMENTAL METHODS

Our experiments were carried out in an ultrahigh-vacuum (UHV) chamber (with a base pressure of at least 5×10^{-11} Torr) equipped with a custom-built NC-AFM operated at RT. The NC-AFM instrument was operated using the frequency modulation detection mode while keeping the cantilever oscillation amplitude constant [44]. Prior to their use in NC-AFM imaging and manipulation experiments, commercial Si cantilevers were carefully cleaned *in situ* via Ar-ion sputtering in a UHV chamber to remove the native oxide layer and other possible contaminations. During data acquisition, an appropriate sample voltage V_s with respect to the grounded tip was applied in order to minimize the long-range electrostatic interactions. Prior to the Si adatom manipulation experiments, force spectroscopic measurements were carried out to characterize the tip-apex chemical reactivity, which was based on the magnitude of the maximum attractive force $F_{\max}$ above the Si adatoms. We used 10 cantilevers with 15 different tip terminations exhibiting different chemical properties (see the distribution of forces and their manipulation capability in Fig. 2 D of Ref. [39]). The tips characterized by larger $F_{\max}$ on adatoms and showing manipulation capability are defined as reactive tips, whereas the tips with smaller $F_{\max}$ and showing no manipulation capability are referred to as less reactive tips [39]. The force spectroscopy measurements were performed by recording the frequency shift Δf with respect to the resonant frequency f_0 as a function of the tip-sample distance z over the selected adatom positions with a lateral precision of 0.1 Å using the atom-tracking method described elsewhere [45]. The measured $\Delta f(z)$ curves can be converted into force-distance curves using the method described in [46]. To quantify the interaction forces and energies with only a short-range contribution, we subtracted the long-range background forces from the total interaction forces acting between the tip and sample. The long-range force contribution is estimated from the $\Delta f(z)$ curve measured above the corner hole site on the Si(111)-(7 × 7) surface.

Manipulation procedure. After compensating for the thermal drift using feedforward control, we performed sequential line scans at constant tip-sample distances along the manipulation path involving a vacancy and a Si adatom in the $[1\bar{1}0]$ direction [see Fig. 1(a)], with the feedback loop interrupted. The achievement of successful atom manipulation requires an accurate adjustment of the scan line above the center of a vacancy and target adatom. This was accomplished using a versatile scan controller [47]. More detailed information on the experimental protocols and manipulation procedure can be found in Ref. [39].

III. RESULTS AND DISCUSSION

We carried out the lateral manipulation of intrinsic Si adatoms on a Si(111)-(7 × 7) surface in the presence of an atomic vacancy as an open space. Because these atom manipulation procedures have been so fully detailed in our previous reports [5,39], we here describe only their general

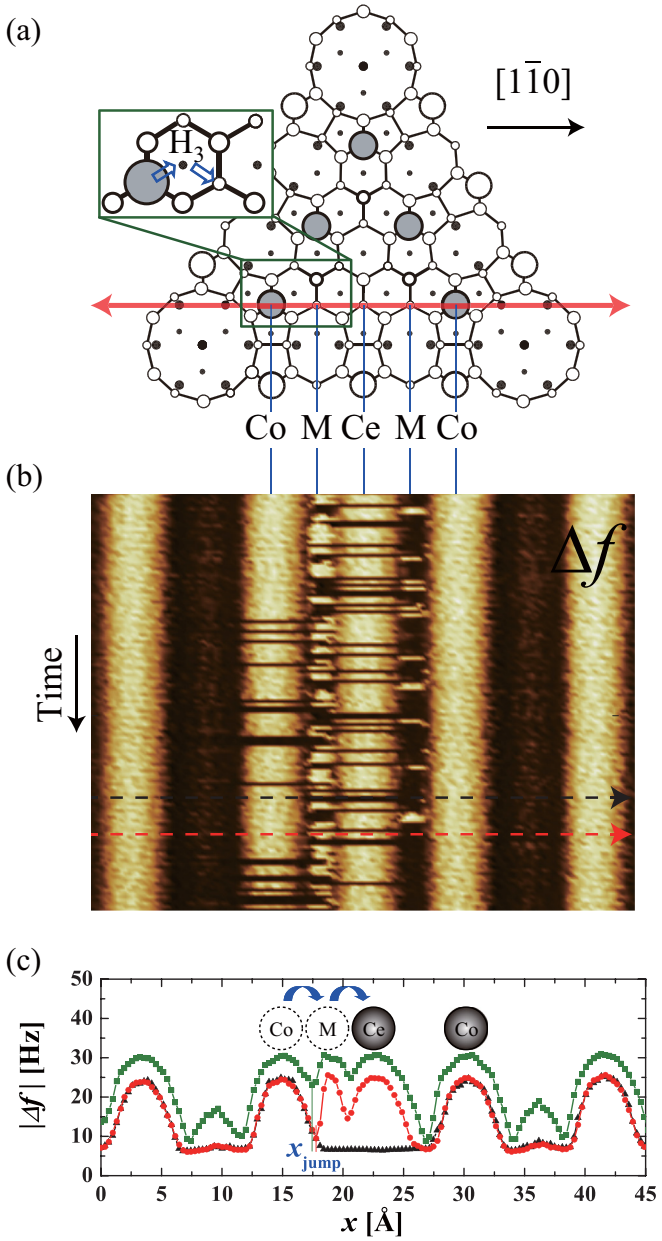

FIG. 1. Lateral manipulation of a Si adatom at constant height via line scans at RT. (a) Schematic top view of a half-unit cell on the Si(111)-(7 × 7) surface involving an atomic vacancy on a center adatom (Ce) site. A detailed view of the most favorable hopping pathway of an adatom located at the corner adatom (Co) site (i.e., Co → H_3 → M transition) is also shown. The red left-right arrow represents the direction of the successive tip scans above the line along the [1$\bar{1}$0] direction involving an atomic vacancy. (b) Constant-height Δf image consisting of a set of sequential line scans along the fast-scan direction passing from left to right, which was recorded with the passage of time at a fixed tip-sample distance z of 1.41 Å. The z values were determined from the force-distance curves acquired over the Si adatoms. (c) Three exemplary Δf line traces extracted from two different Δf image patterns acquired with the same scan parameters at two different tip-sample distances. While the profile indicated with black triangles does not show the atom-hopping signature, the profiles with green squares and red circles show atom hopping from a Co to a Ce site via the M site. The X_{jump} symbol marks the position at which the adatom jumps occur.

features and present results concerning the role of lateral forces on the manipulation process. The atom manipulation process was performed by sequential tip scans along the [1$\bar{1}$0] direction above the surface including an atomic vacancy at the center adatom (Ce) site as schematically shown in Fig. 1(a). This manipulation route was found to be the easiest path for the diffusion of an adatom located on the corner adatom (Co) site towards a vacancy at the Ce site [5]. In order to get statistically reliable results for the atom manipulation process at well-defined distances, the tip was scanned at constant heights without tip-surface distance feedback along the manipulation path while recording the variation in the Δf signal.

In Figure 1(b), we show the resulting constant-height Δf image consisting of a set of consecutive line scans above the same line on the Si(111)-(7 × 7) surface with an atomic vacancy, which was acquired with the passage of time at a tip-sample distance of 1.41 Å. The pattern with bright continuous as well as intermittent stripes in the Δf image indicates the registry of the Si adatom position during the manipulation process. The success and/or failure of the manipulation attempts can be deduced directly from these Δf image patterns and from the associated line profiles, and the location of the atomic jumps can be determined precisely from the extracted Δf line profiles. Three exemplary manipulation profiles extracted from two different Δf image patterns are shown in Fig. 1(c). While the profiles with red circles and black triangles are acquired at the same tip-sample distance with identical manipulation parameters, the profile with green squares was obtained at a closer tip-sample distance. The analysis of the line profiles (black triangles and red circles), taken along the lines highlighted in Δf image shown in Fig. 1(b), reveals two different outcomes of the manipulation process starting from the same initial adatom configuration. While the profile with triangles shows no evidence of adatom displacement and no change in the vacancy at the Ce site, the profile with red circles shows the signature for atom movement. During the tip scanning over the left Co adatom, the Si adatom hops to the M site following the tip motion, leading to an abrupt jump in the Δf signal (at $x = 17.8$ Å). The adatom can then hop from the M site (metastable site) to the Ce site (at $x = 20.7$ Å). After the adatom has jumped to the Ce site, the vacancy is now located on the left Co site.

In order to understand the physical processes responsible for the observed atomic jumps and to reveal the tip dependence of the manipulation process, we performed a statistical analysis of the series of manipulation attempts using various different tips. From the sets of constant-height Δf images acquired at different tip-sample distances and the associated line profiles, we determined the atom-hopping probabilities for different manipulation processes as a function of tip-surface distance. These will be discussed below (further details can also be found in Ref. [39]).

In the following, the role of lateral forces in the manipulation process is revealed by mapping out the force field experienced by the tip over its trajectory along the manipulation pathway connecting the Co to the M site. To quantify the interaction forces acting on the tip when it is located at the lateral positions at which the adatom hopping takes place, we carried out two-dimensional (2D) force mapping experiments with the same tip termination as used

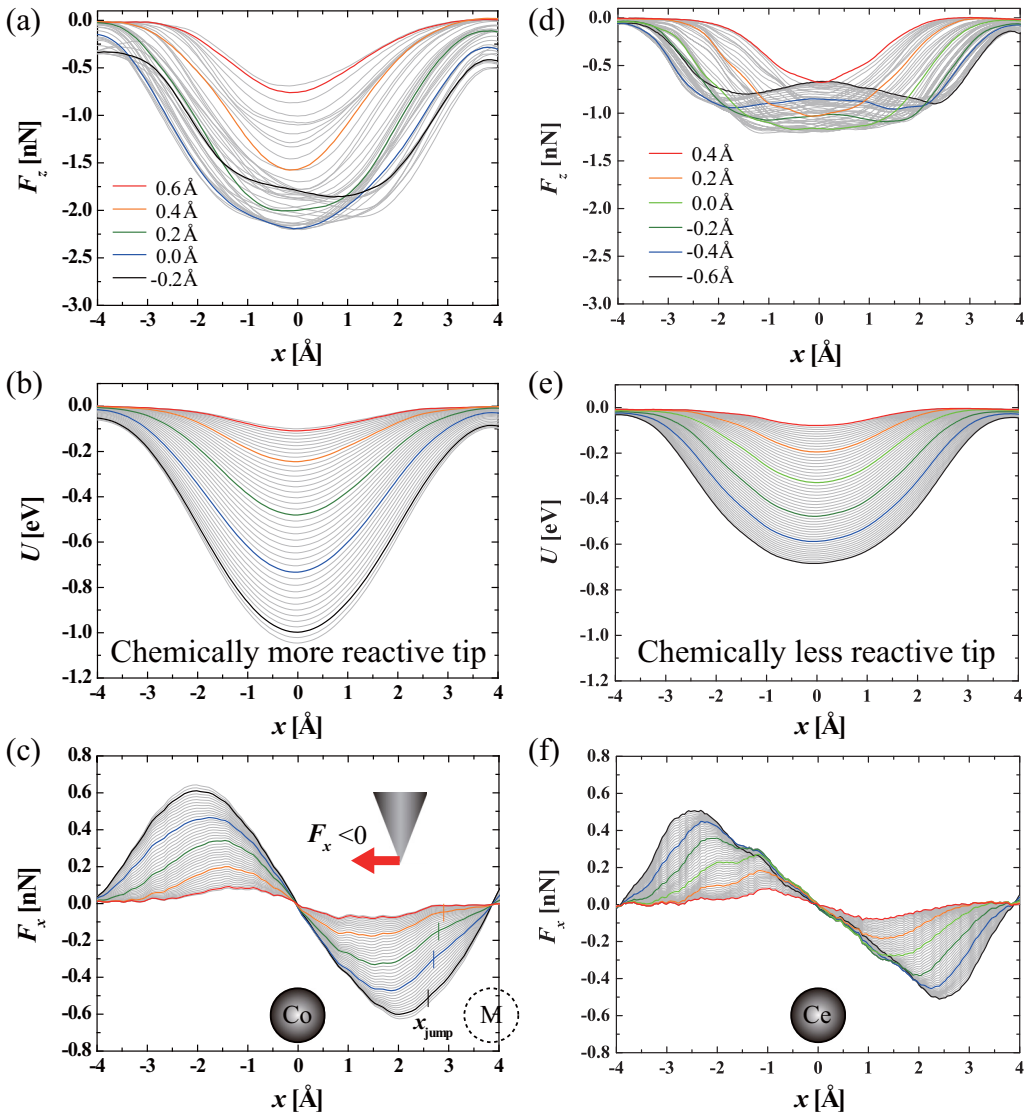

FIG. 2. Vertical and lateral forces as well as interaction energy profiles obtained by moving the tip parallel to the surface at constant height. (a) Vertical force F_z profiles acting on the tip above a Co adatom on a Si(111)-(7 × 7) surface as a function of lateral tip position x obtained for a range of tip-sample separations z, converted from 2D Δf maps acquired with a chemically reactive tip. An asymmetry in the force profiles appears at closer z distances, which might be attributed to the effect of tip asymmetry and/or the structural relaxations in both the tip and surface adatom positions. (b) Tip-adatom interaction energy U profiles, obtained by integration of F_z along the z direction at each x position. (c) The extracted lateral force F_x profiles acting on the tip above a Co adatom, which were obtained by differentiating U with respect to x. The vertical bars indicated in (c) mark the lateral tip positions X_{jump} where atom hopping occurred, as determined from the Δf line profiles shown in Fig. 1(c). (d)–(f) The F_z, U, and F_x profiles acting on the tip above a Ce adatom obtained with a chemically less reactive tip for different tip-sample distances. The numbers in the legends in (a) and (d) denote the z distances of the line scans ($z = 0$, corresponding to the maximum attractive tip-sample force on a Si adatom).

to perform the manipulation experiments shown in Fig. 1. It must be noted here that the same tip-apex termination was also utilized to estimate the atom-hopping probabilities as shown in Figs. 3 and 4(a), which have also been reported in Fig. 2 A of Ref. [39]. Since the interaction force cannot be directly converted from the Δf maps that include the discontinuities of the adatom jumps that occur stochastically at RT, we analyzed the Δf map acquired in a half-unit cell without an atomic vacancy. The difference in the Δf map between two half-unit cells with and without an atomic vacancy was found to be negligibly small for the tip-sample interaction regimes studied here. This was confirmed by the comparison of the force field around an adatom near an atomic vacancy and that around an adatom which does not have a vacancy nearby. Moreover, the similarity of the force fields can also be seen in the Δf line profiles shown in Fig. 1(c) (see the red and black lines). In order to map out the interaction force profile, we acquired constant-height line scans along the Co → M manipulation path as depicted in Fig. 1(a), passing over an adatom located at the Co site. The resulting vertical short-range force F_z and the corresponding tip-sample interaction energy U profiles [48] for a range of tip-sample separations are displayed in

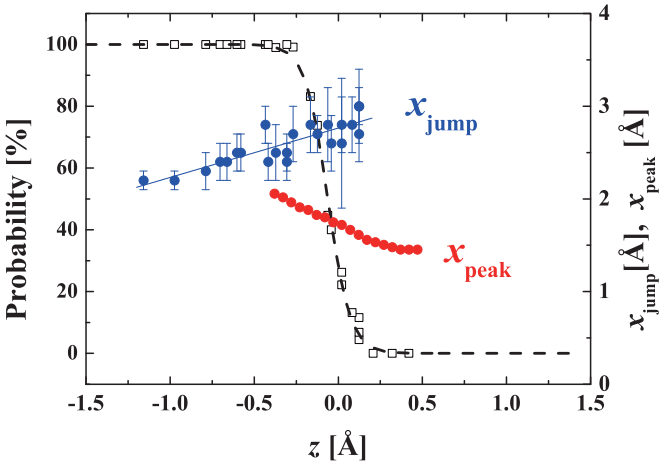

FIG. 3. The average lateral tip positions X_{jump} at which atom hopping from the Co to the M site occurs (blue solid circles), revealing the variation of the X_{jump} values as a function of tip-sample separation z. Note that X_{jump} becomes smaller with decreasing tip-surface separation and approaches the midpoint between Co and M sites; that is, it becomes 1.92 Å. The lateral positions X_{peak} corresponding to the maximum $|F_x|$ values as a function of z are shown by the red solid circles. It is worth noting that X_{jump} values are larger than X_{peak} values for the tip-sample distance ranges explored here. The blue and red solid data points were extracted from Fig. 2(c). The tip-surface distance dependence of the atom-hopping probability from the left Co to the M site is also indicated (black open squares) for comparison [39]. The black dashed line represents the fit to the hopping probability based on an empirical step function. The zero value in the tip-surface distance ($z = 0$) corresponds to the position of the maximum in the F_z (z) curve obtained over the Co adatom site.

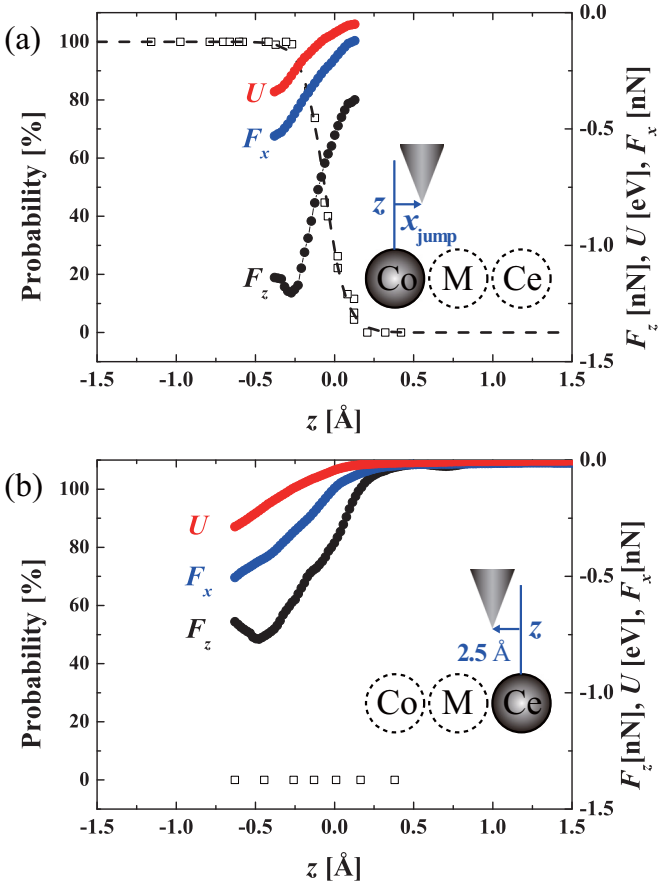

FIG. 4. (a) Distance dependence of F_z, U, and F_x acting on the tip when it was located at the lateral X_{jump} position for the manipulation of a Si adatom from the left Co to the M site (Co $\rightarrow$ M). These data points were extracted from the force and interaction energy profiles shown in Figs. 2(a)–2(c), obtained with a chemically reactive tip. The tip-surface distance dependence of the adatom-hopping probability from the left Co to the M site along the Co $\rightarrow$ M path is also indicated (open black squares) [39]. The black dashed line represents the fit to the hopping probability, which is based on an empirical step function. (b) Distance dependence of F_z, U, and F_x acting on the tip at a lateral tip position shifted from the Ce site by $x = 2.5$ Å, obtained under different tip conditions which did not result in atom movement. The open black squares indicate the atom-hopping probability from the right Ce to the M site as a function of tip-surface distance [39].

Figs. 2(a) and 2(b), respectively. At relatively large tip-sample distances, the F_z profiles indicate a symmetric force minimum over the Co adatom located at $x = 0$. At smaller distances, an asymmetric force profile appears along with a shift in the force minima to the right, which can be attributed to the effect of tip asymmetry and/or the structural relaxations in both the tip and surface atoms [49]. Indeed, we previously observed anisotropic behavior in the manipulation probability using the same tip for two symmetric manipulation pathways of Co to the M site. Namely, the probability from the left Co to the M site was found to be larger than that from the right Co to the M site due to tip asymmetry (see Fig. 2 A in Ref. [39]). Similar observations have been reported previously for the CO manipulation on a Cu(111) substrate [31], where F_z provided by an asymmetric tip apex was found to deviate from circular symmetry above the CO molecule.

We next determined the lateral force F_x profile by differentiating U with respect to x. Figure 2(c) displays the extracted F_x profiles acting on the tip over the Co adatom as a function of the lateral tip position x at different tip-sample separations. Positive and negative signs in the force profiles indicate that the Co adatom pulls the tip to the right and left, respectively. F_x is zero when the tip is located directly over the adatom position, then starts to increase as the tip moves laterally from the Co site until a maximum is reached and vanishes when it is far from the Co adatom site, i.e., at the M site. The lateral tip positions at which the adatom jumps X_{jump} in the course of manipulation attempts are also indicated by the short bars in Fig. 2(c). We determined the X_{jump} positions from the Δf line profiles acquired at different tip-sample separations, as shown in Fig. 1(c). As can be seen in Fig. 2(c), when the tip laterally scans at a constant height from the Co site toward the M site, it passes through the maximum $|F_x|$ position without atom hopping and reaches X_{jump} to induce atom hopping. This is in contrast to the findings of Ternes *et al.* [7] showing that the manipulation occurred at the maximum attractive lateral force for a cobalt atom on the Pt(111) surface and that F_x remained constant while F_z increased below the threshold distances. This implies that the lateral forces do not dominate the manipulation process in our case on semiconductor surfaces. As will be detailed below, this difference can largely be explained in terms of the difference in the electronic structure of the two systems;

the diffusion barrier on low-index metal surfaces is much smaller than that on semiconductors due to the close-packed nature of the metal surfaces compared to the highly corrugated energy landscape on semiconductors.

We also performed the same F_z, U, and F_x mapping experiments using less reactive tips along the same manipulation path to perceive the effect of tip chemical reactivity on the manipulation process [see Figs. 2(d)–2(f)]. The impact of tip reactivity can be clearly realized by a comparison of the interaction energy profiles acquired with reactive [Fig. 2(b)] and less reactive tips [Fig. 2(e)], respectively. A closer look at tip-sample interaction potential maps, which are closely related to the tip-adatom interaction potential, reveals that the reactive tips have a sharper interaction potential profile on the Si adatom than the less reactive tips. A sharper interaction potential profile implies stronger trapping ability of the tip [42], that is to say, a larger force on the adatom. We anticipate that this characteristic property gives tips the ability to locally reduce the energy barrier associated with the Si adatom diffusion, thus enabling adatom hopping toward the tip. Earlier, we demonstrated by means of DFT calculations that the energy barriers associated with Si adatom diffusion can be significantly reduced by the presence of a highly reactive tip [39]. The present findings provide new experimental evidence to explain the reasons behind the ability of reactive tips to locally reduce the energy barrier. Another characteristic feature that can be exploited to distinguish reactive tips from less reactive ones can be inferred from the F_x profiles [see Figs. 2(c) and 2(f)]. A high sensitivity of F_x to distance variation is clearly evident for high-reactivity tips [see Fig. 2(c)]. While the lateral force gradient in proximity to the Co adatom changes with tip-sample distances for a reactive tip, it remains almost constant in the case of a less reactive tip [Fig. 2(f)].

In Fig. 3, we show the lateral tip positions corresponding to the maximum $|F_x|$ values X_{peak} and X_{jump} along with the adatom-hopping probability from the left Co to the M site as a function of tip-sample separations. At large tip-sample distances ($z \geqslant 0.25$ Å), atom-hopping events cannot take place. As the tip approaches the sample surface, the atom-hopping probability increases gradually from 0% at $z \geqslant 0.25$ Å to 100% at $z \leqslant -0.4$ Å. In this stochastic regime, the X_{jump} values (blue solid data points) also fluctuate due to a thermal activation effect. However, the fluctuations in the X_{jump} values decrease as the tip approaches the sample and eventually disappear. This behavior is understandable because at this interaction regime the tip-adatom interaction potential has a relatively shallow minimum, which becomes deeper at closer distances. The relatively weak stabilization of the Si adatom under the tip-trapping potential at the jumping position thus leads to fluctuations in the X_{jump} values. As the tip further approaches the surface, X_{jump} converges to the midpoint between Co and M sites; i.e., X_{jump} becomes 1.92 Å. The most striking result to emerge from the data in Fig. 3, however, is that X_{jump} values are larger than X_{peak} values within the distance ranges analyzed, which means that the lateral force reaches its maximum value before the Co atom jumps to the M site, as previously pointed out.

The results of our analysis for the distance dependence of the vertical and lateral components of the interaction force as well as the interaction energy involved in the manipulation process, acquired with a reactive tip and a relatively less reactive tip, are displayed in Figs. 4(a) and 4(b), respectively. Figure 4(a) shows the tip-sample distance dependence of F_z, U, and F_x acting on the tip when the tip is located at X_{jump} positions for the Co $\rightarrow$ M transition. These values are derived from the 2D maps shown in Figs. 2(a)–2(c). The distance dependence of the adatom-hopping probability from the left Co to the M site along the Co $\rightarrow$ M path is also indicated in Fig. 4(a) for comparison (open black squares). We obtained values of $F_z = -0.65$ nN, $F_x = -0.24$ nN, and $U = -0.11$ eV at $z = -0.06$ Å, which correspond to a hopping probability of 50%. As the tip approaches the surface, the atom-hopping probabilities increased and reached 100% at $z = -0.4$ Å. At $z = -0.4$ Å, we found values of -1.2 nN for F_z, -0.46 nN for F_x, and -0.27 eV for U. In Fig. 4(b), we display the distance dependence of F_z, U, and F_x acting on the tip over the Ce adatom when the tip is located at a fixed lateral position shifted from the Ce adatom by 2.5 Å. This position has been identified as the lateral tip position at which a successful adatom jump is likely to occur with a chemically more reactive tip. Even though the absolute values of $F_z = -0.69$ nN, $F_x = -0.50$ nN, and $U = -0.29$ eV obtained at $z = -0.63$ Å are larger than those obtained at the point corresponding to a hopping rate of 50% in Fig. 4(a), we did not observe any atom manipulation events; that is, atom hopping did not take place. This type of tip belongs to the groups of tips that have no atom manipulation capability. All of this points to the fact that not only the force magnitude but also the extent of the tip chemical reactivity is essential for successful atom manipulation.

Based on the above analysis, we conclude that the lateral forces do not play a decisive role on the lateral manipulation of the Si adatoms on the Si(111)-7 × 7 surface, in contrast to the mechanisms governing the manipulation process on metal surfaces at low temperatures, where lateral forces were found to play a dominant role [7,22]. This difference can be ascribed to the presence of highly directional covalent bonds on semiconductor surfaces [50,51], rather than the nondirectional bonds on metals with strongly extended and delocalized sp-type states [52], which are known to be less sensitive to the hybridization due to the presence of the tip interaction [53]. In the context of NC-AFM, the imaging [54] and manipulation [5] mechanisms on semiconductor surfaces are largely determined by the short-range covalent bonding interactions between the dangling bond at the tip apex and dangling bonds in the surface. The range and the strength of these covalent bonding interactions are generally determined by the alignment of the atomic orbitals at the tip-apex with respect to those of surface atoms. Since a larger tip-adatom force is required to initiate atom movement on semiconductors with a large diffusion barrier (on the order of 1 eV) and large lattice spacing, the detailed atomic structure and chemical nature of the tip-apex are of crucial importance. In this context, the Si-based cluster tips (the H3, T4, and dimer tip structure) with a single dangling bond sticking out of the apex have been shown to reproduce fairly well the short-range chemical forces on Si adatom sites and explain well the atomic-scale features on the semiconductor surfaces [55]. Such a large tip-adatom force required for adatom manipulation can thus be achieved only with a reactive tip with a well-aligned

dangling-bond state with respect to the Si adatoms on the surface. The role of the dangling-bond alignment between the tip and surface adatom on the manipulation capability was previously demonstrated by Jarvis *et al.* [43]. It was revealed that the ability to achieve vertical atom manipulation on semiconductors strongly depends on the orientation of the dangling bonds at the tip apex with respect to the target atom on the surface.

A recent theoretical study demonstrated that structural relaxations in the tip-apex atoms and the following covalent bond formation with the target adatom are essential to the Si adatom displacement [56]. These atomic relaxations enable the formation of covalent bonding interaction even at large tip-sample distances and lead to changes in the orientations of the tip dangling-bond orbitals involved in the manipulation process as well as their charge density distribution; this in turn results in changes in the interaction force components and their sensitivity to the particular manipulation processes. We thus believe that the lack of sensitivity of the manipulation process to lateral force could be explained by the unfavorable orientation of the dangling-bond orbitals between the Si adatoms and the foremost atom of the tip when they are offset from each other at close tip proximity, together with the strong localization of these dangling bonds. Further theoretical studies are needed to provide a better understanding of the observed lack of influence of the lateral force component on the manipulation process.

IV. CONCLUSIONS

We carried out room-temperature lateral manipulation of intrinsic Si adatoms toward a vacancy site on a Si(111)-(7 × 7) surface with the aim of studying the role of lateral forces on the manipulation process. Our results revealed that the lateral forces do not play a decisive role in manipulation processes on semiconductor surfaces and that the vertical interaction force is the key to the manipulation of intrinsic Si adatoms. These findings are in direct contrast to the case for metal substrates. We attribute this difference to the presence of a much larger diffusion energy barrier on semiconductor surfaces due to the strongly localized and highly directional covalent bonds compared to the less corrugated potential-energy landscape on metals. We further addressed the impact of tip chemical reactivity on the manipulation process by examining the force and interaction energy profiles acquired by tips with different degrees of reactivity with Si adatoms. It was found that the chemically more reactive tips present a sharper interaction energy profile on the Si adatom than the chemically less reactive tips, signifying the chemically reactive tips' stronger adatom-trapping ability. This characteristic property gives tips the ability to locally reduce the energy barrier required for adatom displacement, thus enabling adatom hopping toward the tip. These findings can be generally applicable to the manipulation of intrinsic adatoms as well as atomic/molecular adsorbates which are bound strongly to a surface by directional covalent bonds (see, for instance, Ref. [57]) and can thus offer important information in the design of efficient atom manipulation processes on semiconductors and other surfaces with strongly localized dangling-bond states. This information also opens new possibilities for controlling on-surface chemical reactions induced by the mechanical action of a probe.

ACKNOWLEDGMENTS

This work was supported by a Grant-in-Aid for Scientific Research (Grants No. 25106002, No. 16H00959, No. 16H00933, No. 15H03566, No. 16H03872, No. 16K13680, and No. 16K13615) from the Ministry of Education, Culture, Sports, Science and Technology of Japan (MEXT). We also acknowledge financial support from the Murata Science Foundation.

[1] D. M. Eigler, C. P. Lutz, and W. E. Rudge, Nature (London) **352**, 600 (1991).
[2] M. F. Crommie, C. P. Lutz, and D. M. Eigler, Science **262**, 218 (1993).
[3] G. Meyer, S. Zöphel, and K.-H. Rieder, Phys. Rev. Lett. **77**, 2113 (1996).
[4] K. Morgenstern, N. Lorente, and K.-H. Rieder, Phys. Status Solidi B **250**, 1671 (2013).
[5] Y. Sugimoto, P. Jelinek, P. Pou, M. Abe, S. Morita, R. Perez, and O. Custance, Phys. Rev. Lett. **98**, 106104 (2007).
[6] T. Trevethan, L. Kantorovich, J. Polesel-Maris, S. Gauthier, and A. Shluger, Phys. Rev. B **76**, 085414 (2007).
[7] M. Ternes, C. P. Lutz, C. F. Hirjibehedin, F. J. Giessibl, and A. J. Heinrich, Science **319**, 1066 (2008).
[8] Y. Sugimoto, P. Pou, O. Custance, P. Jelinek, M. Abe, R. Perez, and S. Morita, Science **322**, 413 (2008).
[9] Y. Sugimoto, K. Miki, M. Abe, and S. Morita, Phys. Rev. B **78**, 205305 (2008).
[10] O. Custance, R. Perez, and S. Morita, Nat. Nanotechnol. **4**, 803 (2009).
[11] A. Yurtsever, Y. Sugimoto, M. Abe, K. Matsunaga, I. Tanaka, and S. Morita, Phys. Rev. B **84**, 085413 (2011).
[12] A. Sweetman, S. Jarvis, R. Danza, J. Bamidele, S. Gangopadhyay, G. A. Shaw, L. Kantorovich, and P. Moriarty, Phys. Rev. Lett. **106**, 136101 (2011).
[13] Y. Sugimoto, A. Yurtsever, N. Hirayama, M. Abe, and S. Morita, Nat. Commun. **5**, 4360 (2014).
[14] J. Bamidele, S. H. Lee, Y. Kinoshita, R. Turanskŷ, Y. Naitoh, Y. J. Li, Y. Sugawara, I. Štich, and L. Kantorovich, Nat. Commun. **5**, 4476 (2014).
[15] J. Berger, E. J. Spadafora, P. Mutombo, P. Jelinek, and M. Svec, Small **11**, 3686 (2015).
[16] A. Sweetman, I. Lekkas, and P. Moriarty, J. Phys. Condens. Matter **29**, 074003 (2017).
[17] C. Loppacher, M. Guggisberg, O. Pfeiffer, E. Meyer, M. Bammerlin, R. Lüthi, R. Schlittler, J. K. Gimzewski, H. Tang, and C. Joachim, Phys. Rev. Lett. **90**, 066107 (2003).
[18] F. Loske and A. Kühnle, Appl. Phys. Lett. **95**, 043110 (2009).
[19] H. Q. Mao, N. Li, X. Chen, and Q. K. Xue, J. Phys. Condens. Matter **24**, 084004 (2012).

[20] R. Pawlak, S. Fremy, S. Kawai, T. Glatzel, H. Fang, L. A. Fendt, F. Diederich, and E. Meyer, ACS Nano **6**, 6318 (2012).
[21] G. Langewisch, J. Falter, H. Fuchs, and A. Schirmeisen, Phys. Rev. Lett. **110**, 036101 (2013).
[22] S. P. Jarvis, S. Taylor, J. D. Baran, N. R. Champness, J. A. Larsson, and P. Moriarty, Nat. Commun. **6**, 8338 (2015).
[23] J. N. Ladenthin, T. Frederiksen, M. Persson, J. C. Sharp, S. Gawinkowski, J. Waluk, and T. Kumagai, Nat. Chem. **8**, 935 (2016).
[24] S. Hirth, F. Ostendorf, and M. Reichling, Nanotechnology **17**, S148 (2006).
[25] R. Nishi, D. Miyagawa, Y. Seino, I. Yi, and S. Morita, Nanotechnology **17**, S142 (2006).
[26] I. Yi, R. Nishi, M. Abe, Y. Sugimoto, and S. Morita, Jpn. J. Appl. Phys. **50**, 015201 (2011).
[27] S. Torbrugge, O. Custance, S. Morita, and M. Reichling, J. Phys. Condens. Matter **24**, 084010 (2012).
[28] T. Hynninen, G. Cabailh, A. S. Foster, and C. Barth, Sci. Rep. **3**, 1270 (2013).
[29] S. Kawai, A. S. Foster, F. F. Canova, H. Onodera, S.-i. Kitamura, and E. Meyer, Nat. Commun. **5**, 4403 (2014).
[30] G. Langewisch, J. Falter, A. Schirmeisen, and H. Fuchs, Adv. Mater. Interfaces **1**, 1300013 (2014).
[31] M. Emmrich, M. Schneiderbauer, F. Huber, A. J. Weymouth, N. Okabayashi, and F. J. Giessibl, Phys. Rev. Lett. **114**, 146101 (2015).
[32] A. Buldum and S. Ciraci, Phys. Rev. B **54**, 2175 (1996).
[33] U. Kurpick and T. S. Rahman, Phys. Rev. Lett. **83**, 2765 (1999).
[34] A. Kühnle, G. Meyer, S. W. Hla, and K. H. Rieder, Surf. Sci. **499**, 15 (2002).
[35] L. Pizzagalli and A. Baratoff, Phys. Rev. B **68**, 115427 (2003).
[36] T. Trevethan, M. Watkins, L. N. Kantorovich, A. L. Shluger, J. Polesel-Maris, and S. Gauthier, Nanotechnology **17**, 5866 (2006).
[37] A. Deshpande, H. Yildirim, A. Kara, D. P. Acharya, J. Vaughn, T. S. Rahman, and S.-W. Hla, Phys. Rev. Lett. **98**, 028304 (2007).
[38] T. Trevethan, M. Watkins, L. N. Kantorovich, and A. L. Shluger, Phys. Rev. Lett. **98**, 028101 (2007).
[39] Y. Sugimoto, A. Yurtsever, M. Abe, S. Morita, M. Ondráček, P. Pou, R. Pérez, and P. Jelínek, ACS Nano **7**, 7370 (2013).
[40] B. Enkhtaivan and A. Oshiyama, Phys. Rev. B **95**, 035309 (2017).
[41] N. Atodiresei, V. Caciuc, S. Blügel, and H. Hölscher, Phys. Rev. B **77**, 153408 (2008).
[42] Y. Xie, Q. Liu, P. Zhang, W. Zhang, S. Wang, M. Zhuang, Y. Li, F. Gan, and J. Zhuang, Nanotechnology **19**, 335710 (2008).
[43] S. Jarvis, A. Sweetman, J. Bamidele, L. Kantorovich, and P. Moriarty, Phys. Rev. B **85**, 235305 (2012).
[44] T. R. Albrecht, P. Grütter, D. Horne, and D. Rugar, J. Appl. Phys. **69**, 668 (1991).
[45] M. Abe, Y. Sugimoto, O. Custance, and S. Morita, Appl. Phys. Lett. **87**, 173503 (2005).
[46] J. E. Sader and S. P. Jarvis, Appl. Phys. Lett. **84**, 1801 (2004).
[47] I. Horcas, R. Fernandez, J. Gomez-Rodriguez, J. Colchero, J. Gomez-Herrero, and A. Baro, Rev. Sci. Instrum. **78**, 013705 (2007).
[48] Y. Sugimoto, T. Namikawa, K. Miki, M. Abe, and S. Morita, Phys. Rev. B **77**, 195424 (2008).
[49] K. Ruschmeier, A. Schirmeisen, and R. Hoffmann, Phys. Rev. Lett. **101**, 156102 (2008).
[50] Y. Sugimoto, M. Ondráček, M. Abe, P. Pou, S. Morita, R. Perez, F. Flores, and P. Jelínek, Phys. Rev. Lett. **111**, 106803 (2013).
[51] J. Ortega, F. Flores, and A. Levy Yeyati, Phys. Rev. B **58**, 4584 (1998).
[52] M. Ternes, C. Gonzalez, C. P. Lutz, P. Hapala, F. J. Giessibl, P. Jelinek, and A. J. Heinrich, Phys. Rev. Lett. **106**, 016802 (2011).
[53] P. Jelinek, M. Svec, P. Pou, R. Perez, and V. Chab, Phys. Rev. Lett. **101**, 176101 (2008).
[54] R. Perez, M. C. Payne, I. Stich, and K. Terakura, Phys. Rev. Lett. **78**, 678 (1997).
[55] P. Pou, S. A. Ghasemi, P. Jelinek, T. Lenosky, S. Goedecker, and R. Perez, Nanotechnology **20**, 264015 (2009).
[56] B. Enkhtaivan, Y. Sugimoto, and A. Oshiyama, Phys. Rev. B (to be published).
[57] D. L. Keeling, M. J. Humphry, R. H. J. Fawcett, P. H. Beton, C. Hobbs, and L. Kantorovich, Phys. Rev. Lett. **94**, 146104 (2005).